CrossMark

# Magnetic properties and special morphology of barium ferrite via electrospinning

**Gui-Fang Liu, Run-Hua Fan*** , **Zi-Dong Zhang,
Jing Li, Min Chen, Qian-Qian Li, Lu Lu,
Pei-Tao Xie**

**Abstract** Barium ferrite micro-/nanofibers with special morphology, nanowires with diameters of 100 nm, nanoribbons with diameters of 1 μm, and nanotubes with outer diameter of about 300 nm while inner diameter of 100 nm were successfully prepared via electrospinning using different solvents (dimethyl formamide (DMF), solutions of deionized water and ethyl alcohol, and solutions of deionized water and acetic acid, respectively). The barium ferrite micro-/nanofibers were characterized by scanning electron microscope (SEM), X-ray diffraction analysis (XRD), and vibration sample magnetometer (VSM). The results demonstrate that the pure $BaFe_{12}O_{19}$ ferrite phase is successfully formed. And the SEM results show excellent morphologies. The magnetic hysteresis loops demonstrate that their magnetic properties are quite different with different morphologies. The specific saturation magnetization is approximately the same (46.12–49.17 $A·m^2·kg^{-1}$), but the coercivity of the $BaFe_{12}O_{19}$ increases from wires (190.08 $kA·m^{-1}$), ribbons (224.16 $kA·m^{-1}$) to tubes (258.88 $kA·m^{-1}$).

**Keywords** Electrostatic spinning; Barium ferrite; Hollow fiber; Ribbon fiber

G.-F. Liu, R.-H. Fan*, Z.-D. Zhang, J. Li, M. Chen, Q.-Q. Li,
L. Lu, P.-T. Xie
Key Laboratory for Liquid-Solid Structural Evolution and
Processing of Materials, Ministry of Education, Shandong
University, Jinan 250061, China
e-mail: fan@sdu.edu.cn

## 1 Introduction

One-dimensional nanomaterials, including nanowires, nanoribbons, and nanotubes, have many unique properties, such as optical properties, electrical properties, magnetic properties, chemical properties, and some other properties, due to high length–diameter ratio, anisotropy characteristics, and large surface-to-volume ratio. So one-dimensional materials have become one of the research hot spots in the field of nanometer materials in recent years [1, 2].

Up to now, several methods have been used to prepare one-dimensional nanomaterials, such as drawing [3], solvothermal [4], and electrospinning [5]. Among all of these techniques, electrospinning, as a promising method to synthesize nanofibers with large specific surface area and porous structure, attracted much attention. Moreover, it has been applied widely, because it is not only simple to operate and easy to control the operating parameters, but also can be used to obtain uniformly sized large-scale nanofibers with consistent submicron range and produce versatility fibers in a variety of materials (organic materials, inorganic materials, metals, composites, etc.) [6–8], which are difficult to achieve by other techniques. However, there are also some defects of traditional electrospinning, such as the disordered arrange for products, non-uniform in shapes and sizes, and lower productivity, and one of the most serious problems was that the productions were brittle for inorganic non-metallic materials which will limit the application. To solve some of these problems, the electrospun setup was improved. For example, directional collection device was applied to prepare fibers with directional arrangement, and fibers with special morphology were produced. Zhang et al. [1] prepared organic fibers with hollow tubular structure by coaxial electrospinning which can also be used to prepare inorganic hollow fibers,

and this provides a new way of synthesizing inorganic hollow fibers. And with the development of electrospinning, nowadays it has been one of the most important methods in the preparation of a variety of inorganic materials [9–14], such as ZnO and $BaFe_{12}O_{19}$.

A considerable amount of researches were focused on barium ferrites because of their potential applications [15]. So the present work aims to synthesize $BaFe_{12}O_{19}$ hexagonal ferrites with special morphology by a combined technique of electrostatic spinning and high-temperature heating treatment and to investigate the relationship between microstructure and magnetic properties of the samples [16].

To date, there are a few reports on the influence of different microstructures on the magnetic properties of barium ferrites. The materials show that the properties will change as the morphology of materials changes. Many factors can affect the morphology of the fibers via electrospinning, i.e., the properties of the solution (viscosity, concentration, dielectric constant, surface tension, etc.), the operating parameters (voltage, push speed, distance between receiving device and injection device), and environmental factors (temperature, air humidity, etc.). It is believed that the study of special microstructure of barium ferrite is significant and will contribute to expanding the applications of $BaFe_{12}O_{19}$ into the new fields of bio-magnetics and high-density data storage media. In order to achieve better magnetic property and wide-ranging application, in this work, some barium ferrite of special microstructure was fabricated using a combined technique of electrostatic spinning and high-temperature heating treatment [17]. The samples with different morphologies were prepared by changing the experimental conditions. The results exhibited some amazing alterations in structure, morphology and magnetic properties with the change of microstructures [2].

## 2 Experimental

Appropriate amount (a molar ratio of Fe/Ba is 11.5:1.0) of barium nitrate ($Ba(NO_3)_2$, analytical reagent (AR)), and ferric nitrate ($Fe(NO_3)_3\cdot9H_2O$, AR), were dissolved in 20.0 ml dimethyl formamide (DMF), solutions of deionized water and ethyl alcohol was mixed with a volume ratio of 1:4, and solutions of deionized water and acetic acid were also mixed. And then after adding appropriate amount of polyvinylpyrrolidone (PVP) (molecular weight = 1,300,000), the precursor solution was stirred until it became homogeneous transparent brown solution. After laid for about 2 h to eliminate air bubbles in the solution, the stable sol was obtained.

In a typical electrospinning process, the spinneret containing the precursor solution had an inner diameter of about 1 mm. A distance of 15 cm and voltage of 13 kV were maintained between the tip of the spinneret and the collector. After electrospinning, these precursor fibers were first dried in the drying oven in air atmosphere at 80 °C and then calcined at 800 °C for 2 h in a box furnace in air to obtain the fibers with different morphologies [16, 17].

X-ray diffraction (XRD, Rigaku D/max-rB) patterns were collected on a diffractometer with Cu Kα radiation ($\lambda = 0.154$ nm). The morphologies of the samples were investigated by scanning electron microscopy (SEM, SU-70). The magnetic hysteresis loops of the magnets were measured at room temperature using a vibrating sample magnetometer (VSM, JDAW-2000C&D) in applied maximum magnetic field up to 1.2 T [16, 17].

## 3 Results and discussion

### 3.1 Morphological and structural characteristics of products

Figure 1 shows the XRD patterns of barium ferrite with different special microstructures. All the strong diffraction peaks in Fig. 1 can be perfectly indexed as the magneto-plumbite structure for $BaFe_{12}O_{19}$. No other characteristic peaks for impurity are observed in all the three types of fibers. So it can be deduced that the $BaFe_{12}O_{19}$ ferrite phase is successfully formed.

SEM images of the precursor fibers and barium ferrite fibers with different morphologies are shown in Fig. 2. It can be seen that before calcinations, the surfaces of fibers are all smooth, and after calcinations at 800 °C, the fibers remain intact and keep the original morphology, respectively. It also shows that the fibers are indeed composed of many interconnected grains with <100 nm in size. During the thermal treatment, PVP was removed, resulting in a rough surface and a decrease in diameter [18, 19].
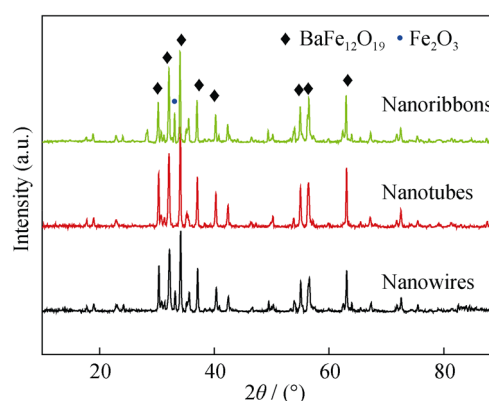


**Fig. 1** XRD patterns of $BaFe_{12}O_{19}$ ferrites with different morphologies
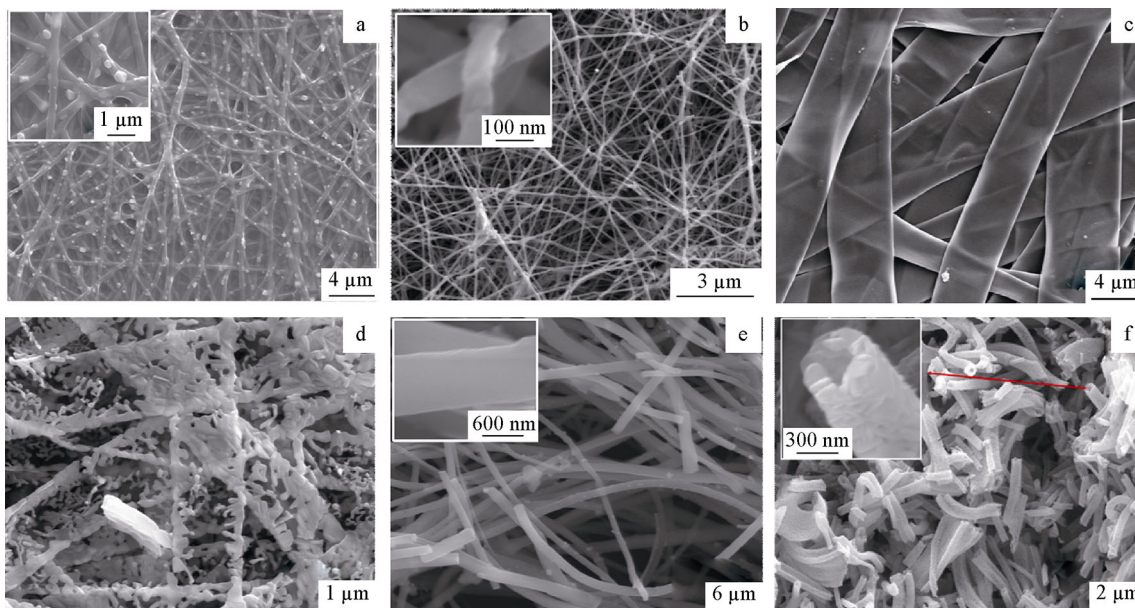
**Fig. 2** Surface SEM images of $BaFe_{12}O_{19}$ ferrites: **a** precursor wires, **b** wires calcined at 800 °C, **c** precursor ribbons, **d** ribbons calcined at 800 °C, **e** precursor tubes, and **f** tubes calcined at 800 °C

Figure 2a, b shows that before calcination, the average diameter of the wires is about 250 nm as obtained via this method, but after calcination, it is about 100 nm. Figure 2c, d shows that before calcination, the width of the ribbons is ranging from 4 to 5 μm, but after calcination, it is about 1 μm. When the solution viscosity of the solution is high, solvent evaporation rate drops. As a result, the fibers collected on the collector are humid and will be evened out on the impact force which is produced when other fibers drop down on the collector, so when the solution is mixed with deionized water and ethyl alcohol with a volume ratio of 1:4 and the viscosity is high, the morphology will be zebraic. As shown in Fig. 2e, f, for the tubes, before calcination, the average diameter of the fibers is about 600 nm, and the hollow structure cannot be observed, but after calcination the hollow structure can be observed clearly; especially, it can be found that the outer diameter is about 300 nm while the inner diameter is 100 nm. The phase separation happens in the polymeric precursor solution as the solution evaporates rapidly. Polymeric precursor solution concentration gradient forms along the radial in the jet processing since the solubilities of the solutions are different. With the continuous volatilization of solvent, hollow fibers are formed spontaneously [20].

## 3.2 Magnetic property of $BaFe_{12}O_{19}$ ferrite fibers

VSM technique was employed to investigate the dynamical magnetic properties of the $BaFe_{12}O_{19}$ fibers. The hysteresis loop measurement was made to determine the magnetic parameters such as the specific saturation magnetization ($M_s$), remanent magnetization ($M_r$) and coercivity ($H_c$). Figure 3 shows typical hysteresis curves of $BaFe_{12}O_{19}$ fibers measured at room temperature. In the hysteresis curves, the ordinate represents the intensity of magnetization ($M$), and the abscissa represents the magnetic field intensity ($H$). And the specific $M_s$, $M_r$, and $H_c$ values of the $BaFe_{12}O_{19}$ ferrite fibers with different morphologies are shown in Table 1, indicating that the coercivity of tubes is 258.88 kA·m$^{-1}$. This value is larger than that of the $BaFe_{12}O_{19}$ wires (190.08 kA·m$^{-1}$) and ribbons (224.16 kA·m$^{-1}$). This curve also shows that the saturated
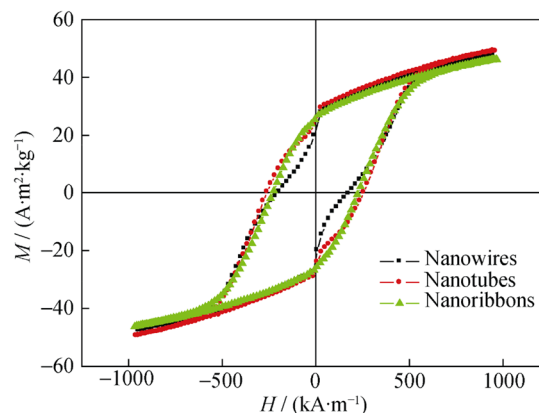


**Fig. 3** Hysteresis loops of $BaFe_{12}O_{19}$ ferrites measured at room temperature

**Table 1** Magnetic properties of $BaFe_{12}O_{19}$

| Samples | $M_s$/ $(A \cdot m^2 \cdot kg^{-1})$ | $M_r$/ $(A \cdot m^2 \cdot kg^{-1})$ | $H_c$/ $(kA \cdot m^{-1})$ | $M_r$/ $M_s$ |
|---------|------|------|------|------|
| Nanowires | 47.120 | 19.23 | 190.08 | 0.41 |
| Nanoribbons | 46.124 | 25.37 | 224.16 | 0.50 |
| Nanotubes | 49.170 | 24.79 | 258.88 | 0.55 |

magnetization ($M_s$) of the $BaFe_{12}O_{19}$ tubes at room temperature is 49.170 $A \cdot m^2 \cdot kg^{-1}$. This value is larger than that of $BaFe_{12}O_{19}$ wires (47.120 $A \cdot m^2 \cdot kg^{-1}$) and ribbons (46.124 $A \cdot m^2 \cdot kg^{-1}$). And the remanent magnetization ($M_r$) of the $BaFe_{12}O_{19}$ tubes at room temperature is 24.79 $A \cdot m^2 \cdot kg^{-1}$. This value is larger than that of $BaFe_{12}O_{19}$ wires (19.23 $A \cdot m^2 \cdot kg^{-1}$) but less than that of ribbons (25.37 $A \cdot m^2 \cdot kg^{-1}$). While the specific saturation magnetization exhibits a behavior different from the specific saturation magnetization ($M_s$), remanent magnetization ($M_r$) and coercivity ($H_c$) [19].

Previous study showed that magnetic parameters of $BaFe_{12}O_{19}$ were concerned with the purity of the samples, the grain sizes, shape, and the arrangement of grains [21]. In this study, $BaFe_{12}O_{19}$ fibers were produced. In the $BaFe_{12}O_{19}$ wires, the small diameter limits the growth of the crystals along radial direction, so crystals can only grow along the fibers axial direction. As a result, the barium ferrite wires are composed of rod-like grains with <100 nm in size, stacking disorderly, rather than hexagonal flake crystals. So the microstructure presents one-dimensional, and it would enhance the anisotropy and improve the coercive force [22]. In the zebraic fibers, the microstructure presents two-dimensional, and in the tube fibers, the microstructure presents three-dimensional. So these structures would reduce the anisotropy to some extent. Furthermore, the magnetic parameters ($M_r$, $H_c$) would reduce in principle. But when the samples were tested, they distribute disorderly, so this could reduce the anisotropy. Finally, it makes the magnetic parameters remain unchanged according to the common rule.

## 4 Conclusion

In this study, barium ferrite micro-/nanofibers with special feature, wires, ribbons, and tubes, were successfully prepared via the electrospinning technique. The fibers form a major phase of barium ferrite. The SEM images show that, before calcinations, the surface of all the three types of fibers is smooth, and after calcinations at 800 °C, the fibers remain intact and keep the original morphology respectively. It also shows that the fibers are indeed composed of many interconnected grains with <100 nm in size. After calcination, the

hollow structure can be observed clearly, the outer diameter is about 300 nm, and the inner diameter is about 100 nm. The ratio of the hollow diameter to the fiber diameter is estimated to be about 1/3. The values of specific saturation magnetization ($M_s$), remanent magnetization ($M_r$), and coercivity ($H_c$) are different as the morphology changes.

## References

[1] Zhang SH, Xu SZ, Dong XT. Preparation and characteristic of hollow PVP nanofibers via electrostatic spinning technique. J Changchun Univ Sci Technol. 2008;30(4):15.

[2] Dai JF, Dai YL, Wang ZX, Gao HF. Preparation and magnetic properties of lanthanum-and cobalt-codoped M-type strontium ferrite nanofibres. J Exp Nanosci. 2015;10(4):249.

[3] Ondarcuhu T, Joachim C. Drawing a single nanofibre over hundreds of microns. Europhys Lett. 1998;42(2):215.

[4] Chen D, Qiao X, Qiu X, Chen J, Jiang R. Convenient synthesis of silver nanowires with adjustable diameters via a solvothermal method. J Colloid Interface Sci. 2010;344(2):286.

[5] Shen X, Liu M, Song F, Meng X. Structural evolution and magnetic properties of $SrFe_{12}O_{19}$ nanofibers by electrospinning. J Sol-Gel Sci Technol. 2010;53(10):448.

[6] Li CJ, Huang BN, Wang JN. Effect of aluminum substitution on microstructure and magnetic properties of electrospun $BaFe_{12}O_{19}$ nanofibers. J Mater Sci. 2013;48(4):1702.

[7] Kim KK, Jin LL. Preparation of PPV nanotubes and nanorods and carbonized products derived there from. Nano Lett. 2001;1(11):631.

[8] Joo J, Park KT, Kim MS. Conducting polymer nanotube and nanowire synthesized by using nanoporous template: synthesis, characteristics and applications. Synth Met. 2003;7(9):135.

[9] Cui QZ, Dong XT, Yu WL. The latest progress of electrostatic spinning technology in the preparation of inorganic nanofibers. Rare Met Mater Eng. 2006;35(7):1167.

[10] Zhang SH, Dong XT, Xu SZ. Preparation and characteristic of $TiO_2@SiO_2$ submicron coaxial cable. J Chem. 2007;65(23):2675.

[11] Dong XT, Wang JX, Cui QZ. Preparation of $LaFeO_3$ porous hollow nanofibers by electrospinning. Int J Chem. 2009;1(1):13.

[12] Shao CL, Guan HY, Liu YC. A novel method for making $ZrO_2$ nanofibres via an electrospinning technique. J Cryst Growth. 2004;267(1–2):380.

[13] Yu HQ, Song HW, Pan GH. Preparation and luminescent properties of $YVO_4$: $Eu^{3+}$ nanofibers by electrospinning. J Nanosci Nanotechnol. 2008;8(3):1432.

[14] Zheng XQ, Fan LJ, Wang JX. Preparation of $ZnFe_2O_4$ nanofibers. J Changchun Univ Sci Technol (Nat Sci Ed). 2009;32(3):403.

[15] El-Sayed SM, Meaz TM, Amer MA. Effect of trivalent ion substitution on the physical properties of M-type hexagonal ferrites. Part Sci Technol. 2014;32(1):39.

[16] Yang YJ, Liu XS, Feng FJ. Effects of barium content on microstructure and magnetic properties of $Sr_{0.7-x}Ba_xLa_{0.3}Fe_{11.8}Zn_{0.2}O_{19}$ M type hexaferrites. Mater Technol Adv Perform Mater. 2014;29(3):189.

[17] Huang BN, Li CJ, Wang JN. Template synthesis and magnetic properties of highly aligned barium hexaferrite ($BaFe_{12}O_{19}$) nanofibers. J Magn Magn Mater. 2013;335:28.

[18] Wang ZJ, Li ZY, Sun JH, Zhang HN, Wang W, Zheng W, Wang C. Improved hydrogen monitoring properties based on p-NiO/n-SnO$_2$ heterojunction composite nanofibers. J Phys Chem C. 2010;114(13):6100.

[19] Song FZ, Shen XQ, Xiang J, Zhu YW. Characterization and magnetic properties of Ba$_x$Sr$_{1-x}$Fe$_{12}$O$_{19}$($x = 0$–1) ferrite hollow fibers via gel-precursor transformation process. J Alloys Compd. 2010;507(1):297.

[20] Lamarck RS. An Introduction to Electrospinning and Nanofibers. In: Mo XM, He CL, Wang HS, editors. Shanghai: Donghua University Press; 2012. 52.

[21] Li QL, Wang YF, Ye Y. Needle-like nano-SrFe$_{12}$O$_{19}$ particles: preparation by sol–gel method and magnetic properties. Chin Inorg Chem. 2008;24(6):907.

[22] Tian Y, Li CJ. Preparation and magnetic research of magnetic rock type Ba$_{0.5}$Sr$_{0.5}$Fe$_{12}$O$_{19}$ nanofibers. Mater Rev Res Paper. 2010;24(9):88.